Planetary-Scale Preconditioning for the Onset of Blocking

STEPHEN J. COLUCCI

Department of Earth and Atmospheric Sciences, Cornell University, Ithaca, New York

(Manuscript received 2 August 1999, in final form 1 August 2000)

ABSTRACT

The local preconditioning of the midtropospheric planetary-scale flow prior to the onset of a blocking episode during January 1985 is investigated. The preconditioned flow is anomalously diffluent, or characterized by anomalously negative planetary-scale, geostrophic stretching deformation. This deformation increases in magnitude with time during the transition to blocking; this tendency in turn is quasigeostrophically forced by the shape of the planetary-scale component of potential vorticity transports. In particular, the planetary-scale component of potential vorticity advection that became increasingly anticyclonic with eastward distance at a rate that increased northward near the block-onset region forced the local planetary-scale flow to become more diffluent prior to blocking. Self-interactions among the synoptic-scale waves and synoptic-to-planetary-scale interactions contributed more importantly than self-interactions among planetary-scale waves to this preconditioning. In the frequency domain, the preconditioning is primarily attributable to the interactions between low- and high-frequency components of the flow, notably to the advection of slowly varying, low potential vorticity by the high-frequency flow.

1. Introduction

Prior to the onset of blocking flow configurations in the atmosphere, a local weakening of the planetary-scale westerlies is often observed. This weakening, thought to be a necessary condition for block onset in atmospheric models (Buizza and Molteni 1996) and in analyses of atmospheric data (Colucci and Alberta 1996), may be interpreted as a preconditioning of the atmospheric flow before there is a local transition to blocking. Planetary-scale westerly flow weakening itself is not necessarily synonymous with blocking, which is often defined, like in this report as will be described below, by the reversal of westerlies to easterlies in the geostrophic wind field.

Climatologically, blocking flows are most frequently observed downstream of the major jet exit regions in the atmosphere, or where there is a diffluent flow field characterized by an eastward decrease in the strength of the geostrophic westerlies. Compare, for example, the mean longitudes of blocks in Colucci and Alberta (1996) with the mean 500-mb height analysis of Blackmon (1976). The interaction between transient, synoptic-scale disturbances and quasistationary, larger-scale diffluent flow fields has been shown to lead to blocking in simple models (e.g., Shutts 1983; Anderson 1995). On the other hand, the interactions of these transients with diffluent flows in jet exit regions are not necessarily followed by blocking.

A common blocking precursor noted by Colucci and Alberta (1996) was the coincidence of weaker than normal planetary-scale (waves 0–7) 500-mb geostrophic westerlies ($u_p' < 0$) with stronger than normal southerly flow ($v_p' > 0$) in the planetary-scale 500-mb geostrophic wind field. These features may be interpreted as being part of the northern branch of an anomalously enhanced diffluent flow field. However, the passage of synoptic-scale transients through this anomalous diffluence, as assessed by the coincidence of $u_p' < 0$, $v_p' > 0$ and intense sea level cyclones, apparently occurs far more frequently than the onset of blocking.

If preconditioning for the onset of blocking is defined by the development of an anomalously enhanced diffluent flow field upstream of the incipient block, then what processes contribute to the formation of the preconditioned flow? The research reported here was motivated by this question.

The approach is to examine in some detail a case of blocking with particular attention focused upon conditions leading to the onset of this block. The selected case occurred during January 1985 and is Atlantic case 8 from the Colucci and Alberta (1996) catalog of blocking cases. A diagnostic model for the development of the anomalous diffluence (preconditioning) will be presented and applied to this case. The contribution from interactions among and between planetary- and syn-

Corresponding author address: Stephen J. Colucci, Department of Earth and Atmospheric Sciences, 1116 Bradfield Hall, Cornell University, Ithaca, NY 14853.
E-mail: sjc25@cornell.edu

© 2001 American Meteorological Society

Downloaded from http://journals.ametsoc.org/doi/pdf/10.1175/1520-0469(2001)058<0933:PSPFTO>2.0.CO;2 by guest on 21 September 2020

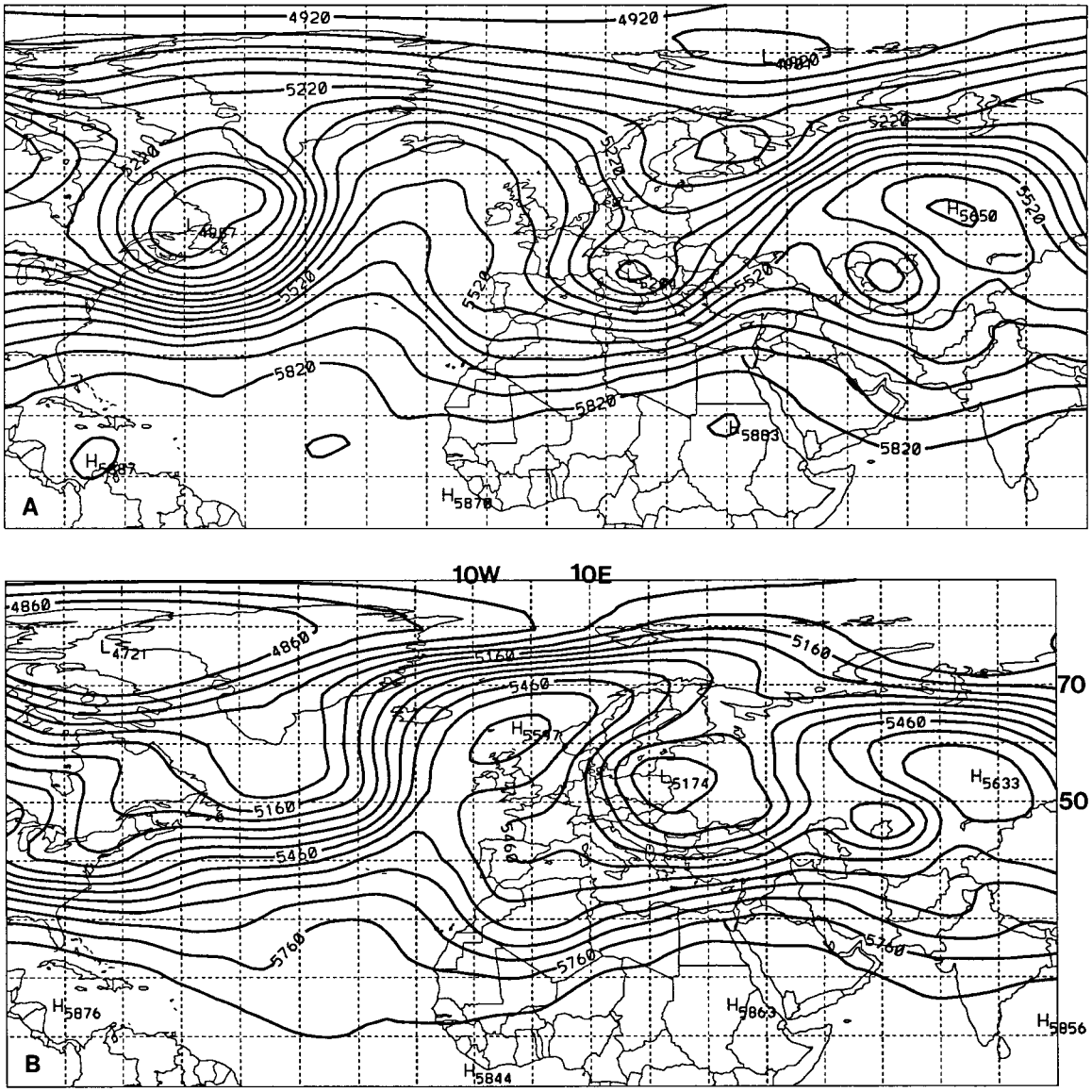

FIG. 1. 500-mb height analyses at (a) 10, (b) 12, and (c) 14 Jan 1985, all times 0000 UTC. The contour interval is 60 m. The latitudes and longitudes marked on (b) define the boundaries for area averages discussed in the text.

optic-scale components of the flow to the preconditioning will be assessed, as well as from interactions among and between low- and high-frequency components of the flow. The results will be interpreted in light of potential vorticity transports in the preblocking environment, yielding new insights on the role of these transports in preconditioning the environment for blocking.

2. The blocking case

Synoptic details and a quasigeostrophic diagnosis of the January 1985 blocking case selected here for further study have been presented by Alberta et al. (1991). Following Colucci and Alberta (1996), we define blocking by the persistence (for at least 5 days) of negative zonal index (500-mb heights higher at 60°N than at 40°N) spanning at least 20 degrees of longitude. Block onset is defined by the first day on which this definition is satisfied for a particular episode. Figure 1 illustrates the transition to blocking in the 500-mb height analyses over western Europe in this case, with block onset on 12 January (Fig. 1b). Notice the anticyclone north of the British isles and geostrophic easterlies (negative zonal index) to the south. The projection of this latter analysis onto the planetary scales (waves 0–7) is shown in Fig. 2. Note the suggestion of planetary-scale geostrophic diffluence near the British Isles on the block onset date.

Colucci and Baumhefner (1998) showed that the formation of this block was preceded in time by the development of a flow pattern characterized by $v_p' > 0$

Downloaded from http://journals.ametsoc.org/doi/pdf/10.1175/1520-0469(2001)058<0933:PSPFTO>2.0.CO;2 by guest on 21 September 2020

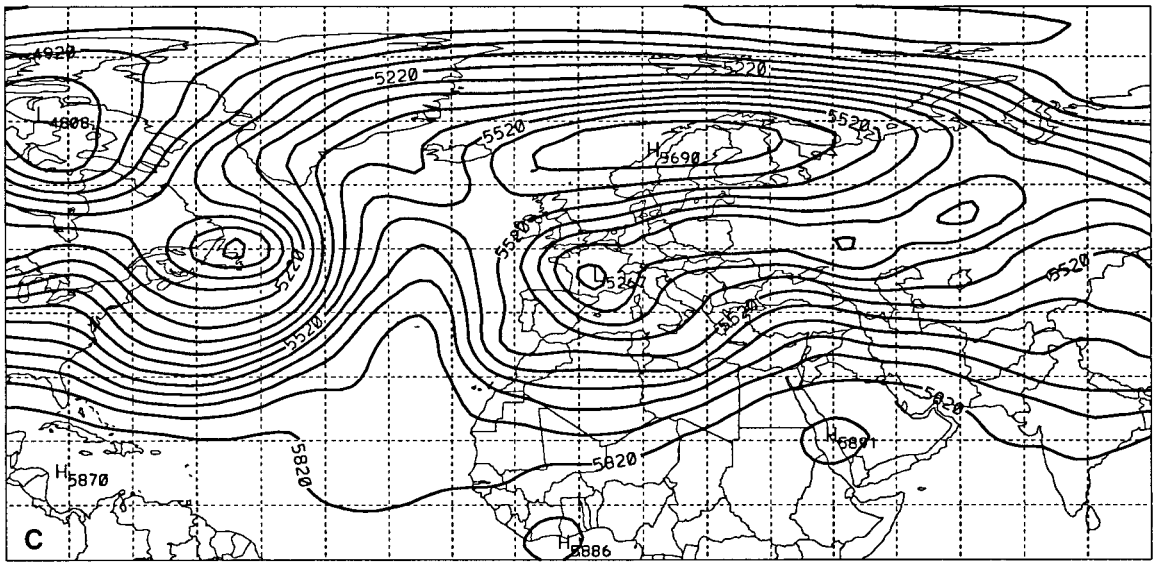

FIG. 1. (*Continued*)

and $u'_p < 0$ at the 500-mb level near the block-onset location. This northern branch of an anomalously diffluent flow field, as described above, may be represented by anomalously negative planetary-scale geostrophic stretching deformation,

$$d'_{1p} = \partial u'_p/\partial x - \partial v'_p/\partial y < 0, \quad (1)$$

which is defined following Mak and Cai (1989) and Bluestein (1992). Here the *p* subscript denotes the planetary-scale (waves 0–7) component, and primes denote a departure from the climatological mean. The evolution of d'_{1p} on the 500-mb level during the 48 h centered on the block-onset date is presented in Fig. 2. These fields were calculated from T42-resolution gridded data of the European Centre for Medium-Range Weather Forecasts as described by Trenberth (1992). The anomalies are departures from 1979–88 mean fields.

Anomalously negative stretching deformation is evident in Fig. 3a near the region of, and one day prior to, block onset. The anomalous 500-mb diffluence locally intensified (i.e., the anomalous planetary-scale stretching deformation became increasingly negative with time) during the 48 h centered on the block-onset date near the developing block. Notice the negative deformation anomaly in Fig. 3b centered near the location of apparent diffluence in Fig. 2. Although the statistical significance of these anomalies has not been assessed, they are locally 50%–100% of the magnitude of the climatological deformation (not shown).

The decrease with time of the planetary-scale geostrophic stretching deformation, averaged around the block-onset region (10°W–10°E, 50°N–70°N) at 500 mb, began four days prior to block onset (Fig. 4). This deformation tendency may thus be considered to be a planetary-scale preconditioning for blocking. The purpose of this work is to therefore seek to identify the processes responsible for the planetary-scale preconditioning (decreasing d_{1p} with time) near the block-onset region.

3. Diagnostic model

Differentiating (1) with respect to time (t) and using the standard definitions of geostrophic wind components, one obtains

$$\partial d_{1p}/\partial t = -2(g/f_0)\partial[\partial(\partial z_p/\partial t)/\partial y]/\partial x, \quad (2)$$

for gravity g, constant Coriolis parameter f_0, planetary-scale component of the geopotential height z_p, and eastward distance x and northward distance y. Note that the primes have been dropped since an anomalous (primed) quantity equals an analysis minus a (constant) climatology, such that the time rate of change of an anomaly equals the time rate of change of the analysis. The planetary-scale deformation tendency is thus proportional to the ''shape'' (x and y derivatives) of the planetary-scale geopotential height tendency field.

A diagnostic equation for the geopotential height (z) tendency field in terms of quasigeostrophic potential vorticity (q) can be written by combining the two terms on the right-hand side (rhs) of Eq. (1) from Alberta et al. (1991) to get:

$$\{\nabla^2 + f_0^2\partial[(1/\sigma)\partial/\partial p]/\partial p\}\partial z/\partial t = -(f_0/g)\mathbf{v}\cdot\boldsymbol{\nabla} q, \quad (3)$$

where σ is the vertically varying static stability, $\mathbf{v}$ is the geostrophic wind, and

$$q = (g/f_0)\nabla^2 z + f + f_0 g\partial[(1/\sigma)(\partial z/\partial p)]/\partial p. \quad (4)$$

Equation (3) is similar to Bluestein's (1992) Eq. (5.8.15), which has a constant static stability parameter. Partitioning the rhs of (3) into planetary- and synoptic-scale contributions allows the height tendency field to be similarly partitioned such that:

Downloaded from http://journals.ametsoc.org/doi/pdf/10.1175/1520-0469(2001)058<0933:PSPFTO>2.0.CO;2 by guest on 21 September 2020

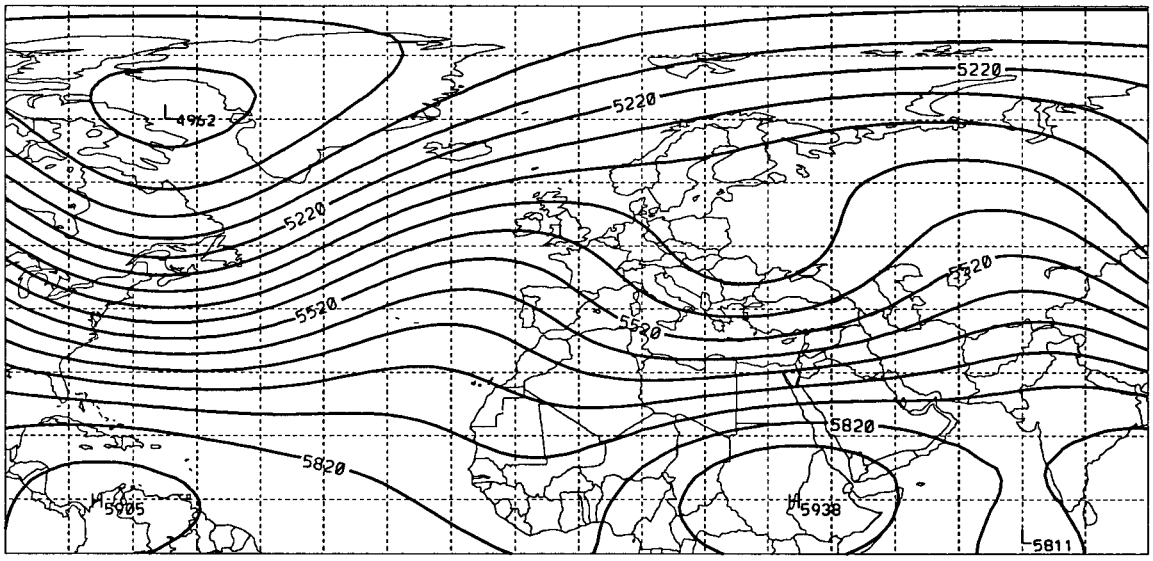

FIG. 2. Planetary-scale (waves 0–7) 500-mb height analysis at 0000 UTC 12 Jan 1985.

$$\{\nabla^2 + f_0^2\partial[(1/\sigma)\partial/\partial p]/\partial p\}\partial z_p/\partial t = -(f_0/g)(\mathbf{v}\cdot\nabla q)_p, \quad (5)$$

$$\{\nabla^2 + f_0^2\partial[(1/\sigma)\partial/\partial p]/\partial p\}\partial z_s/\partial t = -(f_0/g)(\mathbf{v}\cdot\nabla q)_s, \quad (6)$$

where the p subscript denotes contributions from waves 0–7 and the s subscript refers to all other resolvable waves. Henceforth, attention will be focused exclusively on the planetary-scale height tendency equation (5). Differentiation of this equation with respect to x and again with respect to y yields, in combination with Eq. (2):

$$\{\nabla^2 + f_0^2\partial[(1/\sigma)\partial/\partial p]/\partial p\}\partial d_{1p}/\partial t = 2\partial\{\partial[(\mathbf{v}\cdot\nabla q)_p]/\partial y\}/\partial x. \quad (7)$$

By Eq. (7), the planetary-scale geostrophic stretching deformation tendency is related to the shape of the planetary-scale component of the quasigeostrophic potential vorticity advection. Note that $\mathbf{v}\cdot\nabla q$ in the above equation includes contributions from planetary- and synoptic-scale wind and potential vorticity components. It is the projection of this total advection onto the planetary scale that influences the planetary-scale deformation tendency.

Following the standard (e.g., Bluestein 1992) interpretation of equations such as (7) in which the dependent variable on the equation's left-hand side locally has a sign opposite to that of the forcing function on the rhs, then negative planetary-scale geostrophic deformation tendencies are locally associated with a planetary-scale component of quasigeostrophic potential vorticity advection that becomes increasingly anticyclonic $[(\mathbf{v}\cdot\nabla q)_p > 0]$ with northward distance at a rate that increases with eastward distance.

In this work, Eq. (7) was solved by numerical relaxation for the contribution to $\partial d_{1p}/\partial t$ from the forcing function on the RHS of (7). The forcing function and other quantities were calculated from the National Centers for Environmental Prediction (NCEP)–National Center for Atmospheric Research (NCAR) reanalyses of Northern Hemisphere temperatures and geopotential heights (Kalnay et al. 1996) at 10 vertical levels (P = 1000, 925, 850, 700, 500, 400, 300, 250, 200, and 100 mb) on a 2.5° lat by 2.5° long grid. Calculations were performed at 24-h intervals (0000 UTC) during the period of interest (6–15 January 1985). The spectral filtering was accomplished with a spherical harmonic transform (Butkov 1968), retaining zonal and total wavenumbers 0–7. The horizontal finite-differencing schemes accounted for the earth's spherical geometry. The calculated deformation tendencies were set to zero on the upper (100 mb), lower (1000 mb), southern (5°N), and northern (85°N) boundaries. The instantaneously calculated tendencies, at 24-h intervals, were integrated over consecutive time periods to yield calculated 24-h changes in the planetary-scale geostrophic stretching deformation due to the rhs of (7). These were then compared to the analyzed changes in d_{1p} over each 24-h period.

4. Results

The calculated and analyzed changes in d_{1p} over consecutive 24-h intervals during the period of interest, averaged around the block location, are presented in Fig. 5. The calculated and analyzed changes agree qualitatively (in sign) at each interval, but the calculated changes are generally smaller in magnitude. The differences may be due to nonquasigeostrophic processes neglected in the derivation of Eq. (7) as well as to numerical errors. In both the calculations and analyses, the deformation

Downloaded from http://journals.ametsoc.org/doi/pdf/10.1175/1520-0469(2001)058<0933:PSPFTO>2.0.CO;2 by guest on 21 September 2020

decreases are largest in magnitude just prior to block onset.

These calculations suggest that the analyzed decrease in d_{1p} during the transition to blocking over the block-onset region was in this case forced in part by the shape of the planetary-scale component of quasigeostrophic potential vorticity advection. Specifically, the eastward increase in northward-increasing planetary-scale anticyclonic potential vorticity advection over the block onset region helped force the planetary-scale geostrophic deformation to become increasingly negative with time during the transition to blocking. Interpreting the locally decreasing d_{1p} (or increasing planetary-scale geostrophic diffluence) as the preconditioning for this blocking case, then the results imply that this preconditioning was forced in part by the shape of the planetary-scale component of the quasigeostrophic potential vorticity advection near the developing block.

5. Scale interactions in block preconditioning

There has been considerable interest in the relevance of scale interactions to blocking (e.g., Hansen and Chen 1982; Tracton 1990; Lupo and Smith 1995). The importance of these interactions during the preconditioning phase of the blocking case under study was assessed as follows. First, planetary-scale geopotential height fields, z_p, were calculated through spectral filtering of the height fields, as described above. Synoptic-scale geopotential height fields, z_s, were then calculated as differences between the analyzed and planetary scale height fields, or $z_s = z - z_p$. Using Eq. (4), planetary- and synoptic-scale potential vorticity fields (q_p and q_s) were calculated from z_p and z_s, respectively. In a similar fashion, planetary- and synoptic-scale geostrophic wind fields ($\mathbf{v}_p$ and $\mathbf{v}_s$) were calculated. Since $\mathbf{v} = \mathbf{v}_p + \mathbf{v}_s$ and $q = q_p + q_s$, then

$$\mathbf{v}\cdot\nabla q = \mathbf{v}_p\cdot\nabla q_p + \mathbf{v}_p\cdot\nabla q_s + \mathbf{v}_s\cdot\nabla q_p + \mathbf{v}_s\cdot\nabla q_s. \quad (8)$$

The first term on the rhs of (8) represents the self-interaction among the planetary-scale waves, the middle two terms represent the interaction between the synoptic- and planetary-scale waves, and the last term represents the self-interaction among the synoptic-scale waves.

Substitution of (8) into (7) allows Eq. (7) to be partitioned into four equations, each involving one of the interactions on the rhs of (8). Each of these equations was then numerically solved, following the procedure detailed above, to obtain the contribution to the planetary-scale quasigeostrophic stretching deformation tendency field from each of the interactions on the rhs of Eq. (8). The resulting fields were numerically integrated over time to yield calculated, 24-h scale-interaction tendencies, following the procedure discussed earlier for presenting calculated and analyzed deformation tendencies. Finally, at each time period, the fields were averaged over 50°–70°N and 10°W–10°E, which encloses the 500-mb anticyclone in Fig. 1b. The resulting averages at 500 mb are presented in Table 1, where contributions from the middle two terms on the rhs of Eq. (8) are added to form one synoptic-to-planetary-scale interaction effect. The analyzed and total calculated (quasigeostrophic) deformation changes from Fig. 5 are also shown here for comparison. Added together, the contributions from the interactions do not exactly yield the total calculated tendency because of numerical errors.

It is clear from Table 1 that no single interaction process dominated the others throughout the blocking case. Of particular interest are the contributions to the analyzed negative deformation tendencies at time periods 3–7 (8–9 through 12–13 January). Recalling that block onset was on 12 January in this case, then periods 3–5 may be regarded as the ''preconditioning phase'' of this blocking case, while periods 6–7 may be viewed as the ''onset phase.'' First, self-interactions among the synoptic-scale waves, then interactions between planetary- and synoptic-scale waves, appeared to contribute more importantly than self-interactions among the planetary-scale waves to the preconditioning. The contribution to the deformation tendency from the self-interactions among the planetary-scale waves was generally small throughout this episode until the onset phase.

Of the two terms representing in Eq. (8) the synoptic-to-planetary-scale interactions, the second term on the rhs (advection of synoptic-scale potential vorticity by the planetary-scale flow) contributed more importantly to the deformation tendencies throughout the blocking episode (not shown). At most time periods the deformation change due to this effect was of the same sign as the analyzed deformation change.

From these results and those presented in the preceding section, it appears that the preconditioning of the planetary-scale environment (decreasing planetary-scale stretching deformation) prior to this blocking case was due primarily to the effects of synoptic-to-planetary-scale interactions and self-interactions among the synoptic-scale waves. These interactions are represented by the last three terms on the RHS of Eq. (8). Their effects on the deformation field are manifested through the shape of the planetary-scale projection of these interactions, following the interpretations above. Specifically, a planetary-scale component of anticyclonic potential vorticity advection involving these interactions and increasing eastward at a northward-increasing rate helped force the planetary-scale stretching deformation to locally decrease with time in this case.

6. Frequency component interactions

Likewise, there has been considerable interest in the relative importance of low- and high-frequency components of the flow and interactions between them in blocking developments. For example, Nakamura et al. (1997) found that low (high) frequency processes were

Downloaded from http://journals.ametsoc.org/doi/pdf/10.1175/1520-0469(2001)058<0933:PSPFTO>2.0.CO;2 by guest on 21 September 2020

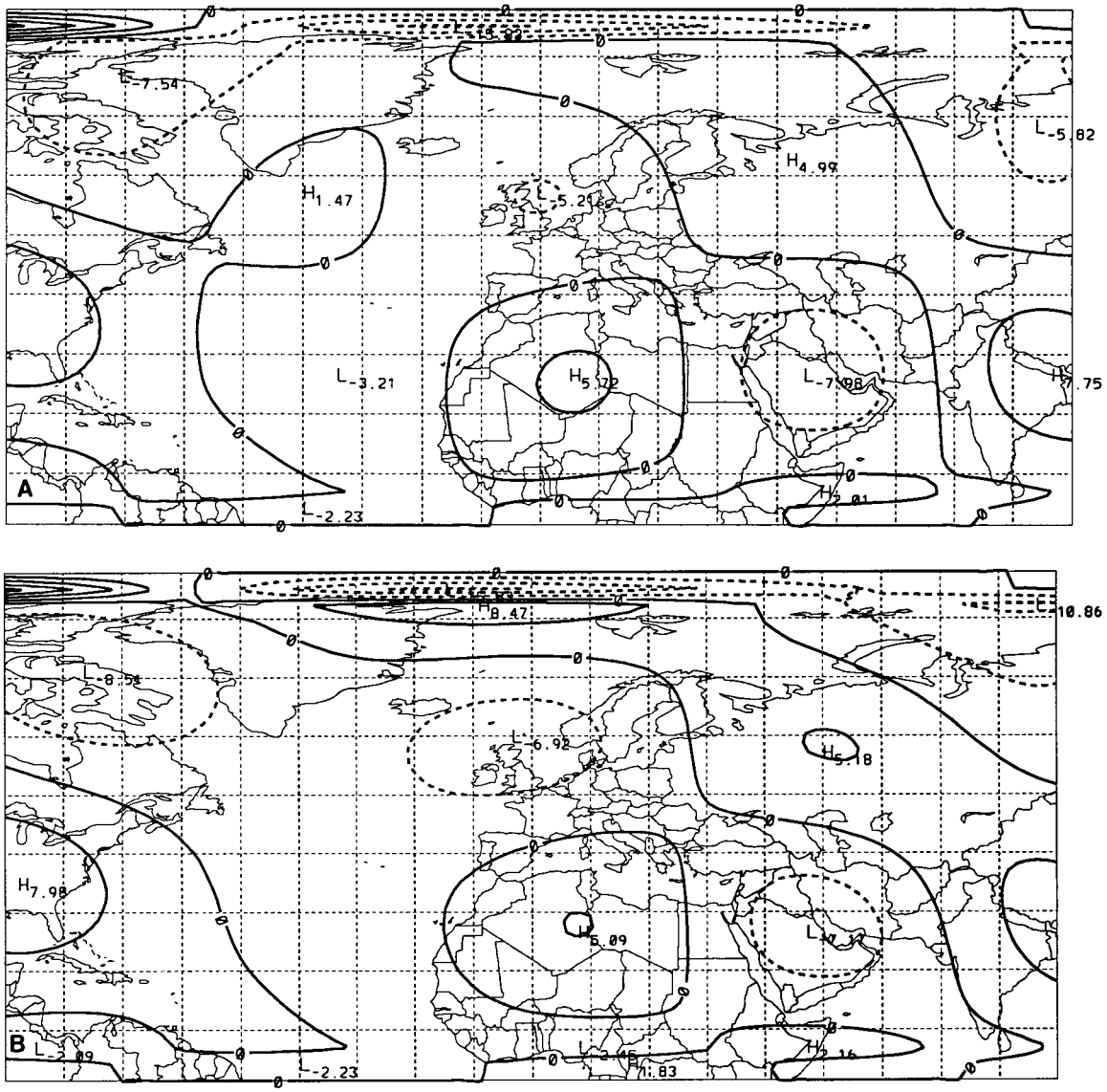

FIG. 3. Anomalous planetary-scale geostrophic stretching deformation at 500 mb on (a) 11, (b) 12, and (c) 13 Jan 1985, all times 0000 UTC. The contour interval is 5×10^{-6} s^{-1} and dashed contours are negative.

relatively more important during the evolution of Atlantic (Pacific) blocking episodes. It would thus be worthwhile to investigate the contribution of processes at different frequencies to the deformation tendencies associated with block preconditioning.

Following Mak (1991), the low-frequency (L) component of an atmospheric variable on a particular day is defined here by the 11-day mean of that variable centered on that day. The high-frequency (H) component of that variable is then the difference between the analysis and low-frequency component of that variable. With these definitions, Eq. (8) may be rewritten as

$$\mathbf{v} \cdot \nabla q = \mathbf{v}_L \cdot \nabla q_L + \mathbf{v}_L \cdot \nabla q_H + \mathbf{v}_H \cdot \nabla q_L + \mathbf{v}_H \cdot \nabla q_H. \quad (9)$$

The first and last terms on the rhs of Eq. (9) represent, respectively, the self-interactions among the low- and high-frequency components of the flow, while the two middle terms represent interactions between low- and high-frequency flow components. Following the procedure described above, the contributions of these terms to the total quasigeostrophic deformation changes were calculated during the event of interest and are presented in Table 2.

The striking feature of Table 2 is the dominance of the contribution from low-to-high-frequency interactions at each time period during the blocking episode. Not only is this contribution larger in magnitude than that from the self-interactions among low- and high-frequency components, but it agrees in sign at each time period with the sign of the analyzed deformation change.

Downloaded from http://journals.ametsoc.org/doi/pdf/10.1175/1520-0469(2001)058<0933:PSPFTO>2.0.CO;2 by guest on 21 September 2020

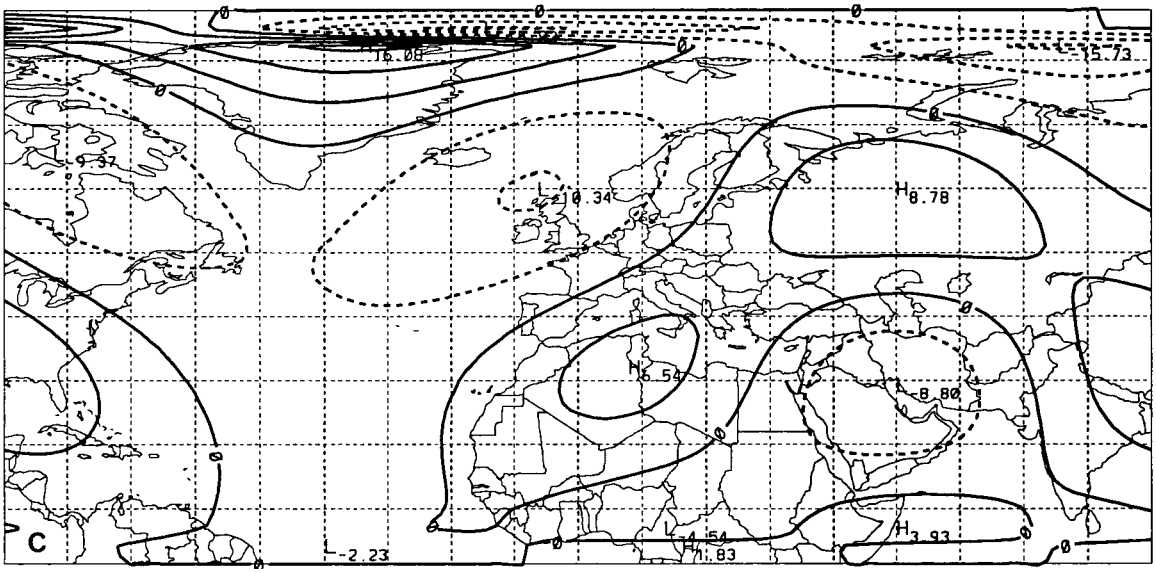

FIG. 3. (*Continued*)

Interestingly, the third term on the rhs of Eq. (9), the advection of low-frequency potential vorticity by the high-frequency component of the flow, contributed more importantly than does the second term on the rhs of Eq. (9) to this low-to-high-frequency interaction effect at most time periods, notably during the ''preconditioning'' phase (periods 3–5) of the blocking episode (not shown). Nielsen-Gammon and Lefevre (1996) have discussed this process in the context of geopotential height tendencies during trough formation and have associated it with ''downstream development'' (Orlanski and Chang 1993).

Inspection of daily 500-mb analyses (not shown) of low-frequency potential vorticity and high-frequency geopotential height during the preconditioning phase reveals a persistent and slowly varying lobe of low potential vorticity west of the block-onset region coupled with a region of negative high-frequency geopotential

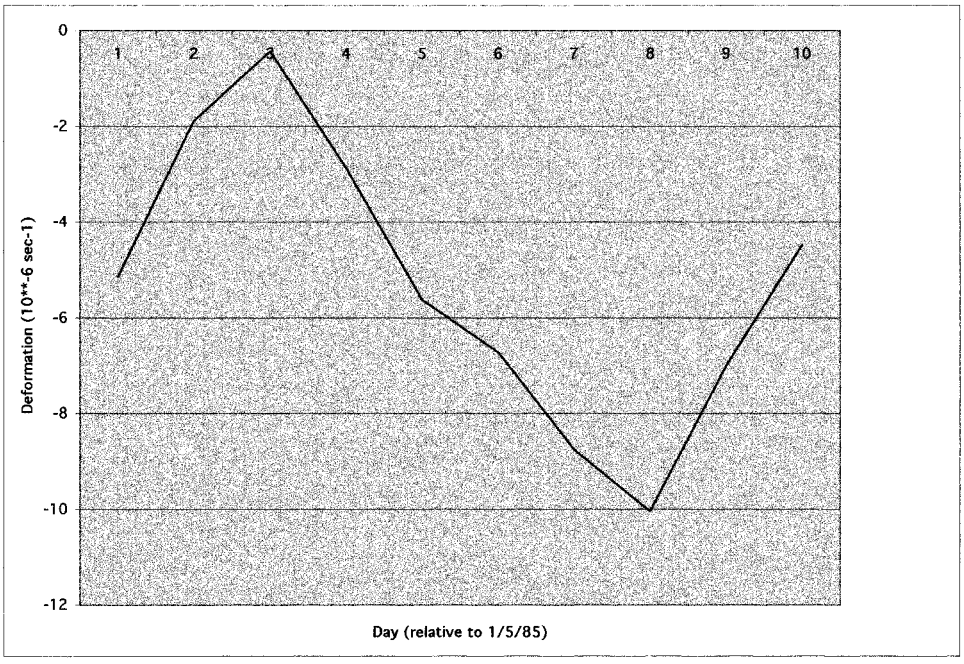

FIG. 4. Planetary-scale geostrophic stretching deformation (10^{-6} s^{-1}), averaged over the block-onset region (50°–70°N and 10°E–10°W) at 500 mb, as a function of day relative to 0000 UTC 5 Jan 1985. The block onset is on day 7 (0000 UTC 12 Jan 1985).

Downloaded from http://journals.ametsoc.org/doi/pdf/10.1175/1520-0469(2001)058<0933:PSPFTO>2.0.CO;2 by guest on 21 September 2020

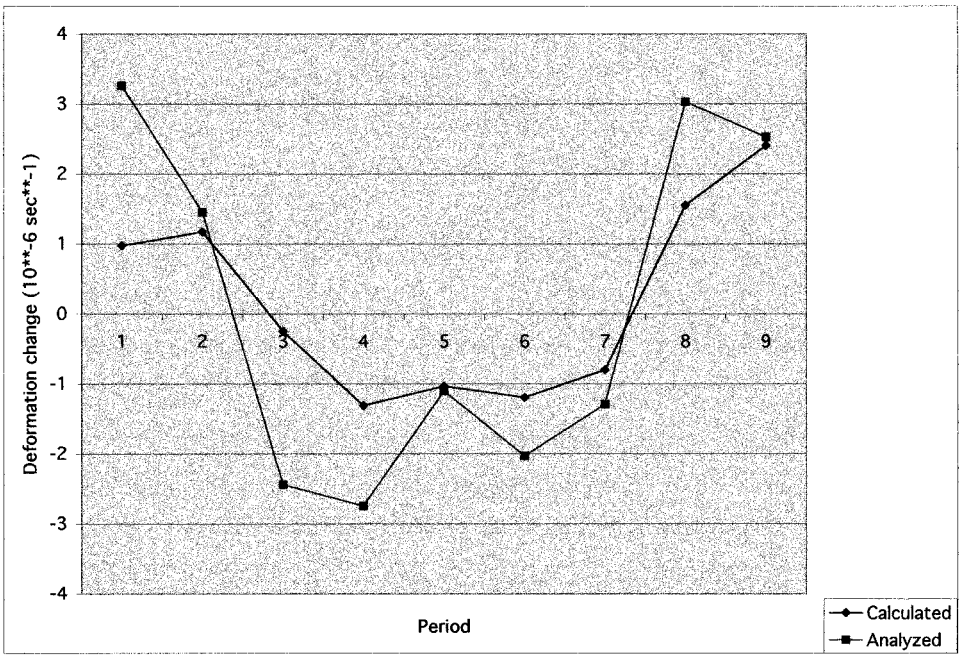

FIG. 5. Analyzed (squares) and total calculated (triangles) changes in the planetary-scale geostrophic stretching deformation (10^{-6} s^{-1}), averaged over the block-onset region (50°–70°N and 10°E–10°W) at 500 mb, during 24-h periods beginning with 0000 UTC 6–0000 UTC 7 Jan 1985 (period 1). The block-onset day (0000 UTC 12 Jan 1985) is between periods 6 and 7.

height just north of this region. This latter feature induced high-frequency westerly flow advecting low-frequency potential vorticity into the block-onset region. The shape of the planetary-scale projection of this advection, increasing eastward at a northward-increasing rate, forced the planetary-scale stretching deformation to locally decrease with time over the block-onset region, by earlier arguments.

This result may be reconciled with the previously presented scale-interaction interpretation as follows. During the block preconditioning phase, the planetary-scale flow advected synoptic-scale anticyclonic potential vorticity across the block-onset region; the shape of the planetary-scale projection of this advection helped force the deformation tendencies associated with the preconditioning. This advection apparently also forced to its north high-frequency westerly flow, which advected low-frequency anticyclonic potential vorticity into the block-onset region; the shape of the planetary-scale projection of this advection also helped force the deformation tendencies linked to the preconditioning. The anomalous planetary-scale diffluence that locally developed prior to the onset of this block was thus primarily forced by the advection of slowly varying, low potential vorticity by high-frequency flow that in turn

TABLE 1. Twenty-four-hour changes in the 500-mb planetary-scale geostrophic stretching deformation (10^{-6} s^{-1}) due to self-interactions among the planetary-scale waves (PP), synoptic-planetary-scale interactions (SP), and self-interactions among the synoptic-scale waves (SS), averaged over 50°–70°N and 10°W–10°E. Also shown are the total analyzed (TA) and total quasigeostrophic (TQ) area-averaged deformation changes. Days are during Jan 1985.

Period	Days	TA	TQ	PP	SP	SS
1	6–7	3.3	1.0	0.0	1.5	−0.2
2	7–8	1.5	1.1	0.1	1.3	0.1
3	8–9	−2.4	−0.2	0.2	0.5	−0.8
4	9–10	−2.7	−1.3	0.4	−0.6	−0.9
5	10–11	−1.1	−1.0	−0.1	−0.9	−0.1
6	11–12	−2.0	−1.2	−0.4	−0.9	0.1
7	12–13	−1.3	−0.8	−0.8	0.0	0.3
8	13–14	3.0	1.6	−0.7	2.2	−0.4
9	14–15	2.5	2.4	−0.6	3.1	0.3

TABLE 2. Twenty-four-hour changes in the 500-mb planetary-scale geostrophic stretching deformation (10^{-6} s^{-1}) due to self-interactions among the low-frequency components (LL), low-high-frequency component interactions (LH), and self-interactions among the high-frequency components (HH), averaged over 50°–70°N and 10°W–10°E. Also shown are the total analyzed (TA) and total quasigeostrophic (TQ) area-averaged deformation changes. Days are during Jan 1985.

Period	Days	TA	TQ	LL	LH	HH
1	6–7	3.3	1.0	−0.2	0.7	0.2
2	7–8	1.5	1.1	−0.2	1.1	0.1
3	8–9	−2.4	−0.2	−0.1	−0.1	−0.1
4	9–10	−2.7	−1.3	0.1	−1.4	−0.1
5	10–11	−1.1	−1.0	0.2	−1.7	0.1
6	11–12	−2.0	−1.2	0.3	−1.8	0.2
7	12–13	−1.3	−0.8	0.3	−1.1	−0.1
8	13–14	3.0	1.6	0.3	1.1	0.3
9	14–15	2.5	2.4	0.2	1.3	0.6

Downloaded from http://journals.ametsoc.org/doi/pdf/10.1175/1520-0469(2001)058<0933:PSPFTO>2.0.CO;2 by guest on 21 September 2020

was apparently induced by the advection of synoptic-scale anticyclonic potential vorticity by the planetary-scale flow. This interpretation is speculative, however, and needs to be confirmed with additional calculations.

7. Discussion

In the case studied, the onset of blocked flow (persistent, large-scale geostrophic easterlies in the midlatitude middle troposphere) was locally preceded in time by the development and intensification of anomalously negative planetary-scale geostrophic stretching deformation. This preconditioned, diffluent flow was forced in this case by the shape of the planetary-scale component of potential vorticity transports. These transports have been implicated in block onsets by many observational and modeling studies (e.g., Nakamura et al. 1997; de Pondeca et al. 1998, and references therein), including studies of this particular blocking case (Colucci and Alberta 1996; Colucci and Baumhefner 1998).

A spectral decomposition of the potential vorticity transports in this case revealed that those transports involving synoptic-to-planetary-scale interactions and self-interactions among the synoptic-scale waves contributed more importantly than self-interactions among the planetary-scale waves to the quasigeostrophic change in planetary-scale stretching deformation during the preconditioning phase of this blocking episode.

The role of these transports in the preconditioning for this blocking case can be interpreted as follows. The advection of anticyclonic potential vorticity on a constant pressure surface is locally associated with geopotential height rises on that pressure surface, by Eq. (3). If this potential vorticity advection projects stongly onto the planetary scales, then, by Eq. (5), it will locally force planetary-scale geopotential height rises. Furthermore, if this planetary-scale component of anticyclonic potential vorticity advection near a point increases toward the north at a rate that increases eastward, then the planetary-scale geopotential height rises will vary horizontally in a similar fashion. In other words, $\partial[\partial(\partial z_p/\partial t)/\partial y]/\partial x > 0$. This horizontal structure, by (2), causes the planetary-scale geostrophic stretching deformation to become more negative (i.e., flow to become more diffluent) near that point. Physically, this structure implies that the westerly component of the planetary-scale geostrophic wind $[-(g/f_0)\partial z_p/\partial y]$ weakens with eastward distance near the point, and this weakening increases in magnitude with time. Alternatively, the southerly component of this wind $[(g/f_0)\partial z_p/\partial x]$ increases with northward distance, and this northward increase also increases with time. However it is viewed, this process renders the planetary-scale flow more diffluent near the reference point.

A temporal decomposition of the potential vorticity transports identified a forcing by interactions between low- and high-frequency components of the flow, notably advection of slowly varying, low potential vorticity by high-frequency flow, in the block preconditioning. A possible link between these frequency interactions and the above-mentioned scale interactions was proposed but needs further investigation.

These results have important implications for the numerical prediction of blocking by operational forecasting and general circulation models. It is well known that these models underpredict the frequency of blocking (e.g., Colucci and Baumhefner 1998; Watson 1999). A possibly related feature of these models is their bias toward excessively zonal flow, especially over regions typically characterized by blocking. Such flows may be insufficiently diffluent and therefore inadequately preconditioned for block onset. The methodology employed in the present study of an analyzed block could be applied to numerical model output in order to diagnose the sources of error leading to improperly preconditioned flow fields prior to misforecast blocks.

Since the conclusions reported herein pertain to a single analyzed blocking case, their generality is unknown. It would be worthwhile to determine if anomalously negative planetary-scale stretching deformation in the middle troposphere is a typical signature of analyzed block onsets, and if the absence or underprediction of this feature in a numerical model's forecast portends a misforecast block by that model. It would also be useful to learn if the particular scale and frequency-band interactions identified in the case studied here are as relevant to other analyzed block-onset cases as they were to this specific case. The origin of the features contributing to these interactions, such as the slowly varying low potential vorticity, synoptic-scale anticyclonic potential vorticity, and high-frequency westerly flow should be determined in this case and in others where they are relevant. These issues will be subsequently investigated.

Acknowledgments. This work was supported in part by National Science Foundation (NSF) Grant ATM-9726250. The ECMWF data were acquired through resources provided by the Scientific Computing Division of NCAR, which is supported by NSF. The NCEP–NCAR reanalysis data were accessed through the Web site http://www.cdc.noaa.gov/cdc/data.nmc.reanalysis.html#pressure of the National Oceanographic and Atmospheric Administration's Climate Diagnostic Center. The reviewers are thanked for making helpful suggestions for improvements to this manuscript.

REFERENCES

Alberta, T. L., S. J. Colucci, and J. C. Davenport, 1991: Rapid 500-mb cyclogenesis and anticyclogenesis. *Mon. Wea. Rev.,* **119,** 1186–1204.

Anderson, J. L., 1995: A simulation of atmospheric blocking with a forced barotropic model. *J. Atmos. Sci.,* **52,** 2593–2608.

Blackmon, M. L., 1976: A climatological spectral study of the 500-mb geopotential height of the Northern Hemisphere. *J. Atmos. Sci.,* **33,** 1607–1623.

Downloaded from http://journals.ametsoc.org/doi/pdf/10.1175/1520-0469(2001)058<0933:PSPFTO>2.0.CO;2 by guest on 21 September 2020

Bluestein, H. B., 1992: *Synoptic-Dynamic Meteorology in Midlatitudes.* Vol. 1. Oxford University Press, 431 pp.

Buizza, R., and F. Molteni, 1996: The role of finite-time barotropic instability during the transition to blocking. *J. Atmos. Sci.,* **53,** 1675–1697.

Butkov, E., 1968: *Mathematical Physics.* Addison-Wesley Publishing Company, 735 pp.

Colucci, S. J., and T. L. Alberta, 1996: Planetary-scale climatology of explosive cyclogenesis and blocking. *Mon. Wea. Rev.,* **124,** 2509–2520.

——, and D. P. Baumhefner, 1998: Numerical prediction of the onset of blocking: A case study with forecast ensembles. *Mon. Wea. Rev.,* **126,** 773–784.

de Pondeca, M. S. F. V., A. Barcilon, and X. Zou, 1998: The role of wave breaking, linear instability and PV transports in model block onset. *J. Atmos. Sci.,* **55,** 2852–2873.

Hansen, A. R., and T.-C. Chen, 1982: A spectral energetics study of atmospheric blocking. *Mon. Wea. Rev.,* **110,** 1146–1165.

Kalnay, E., and Coauthors, 1996: The NCEP/NCAR 40-Year Reanalysis Project. *Bull. Amer. Meteor. Soc.,* **77,** 437–471.

Lupo, A. R., and P. J. Smith, 1995: Planetary and synoptic-scale interactions during the life cycle of a mid-latitude blocking anticyclone over the North Atlantic. *Tellus,* **47,** 575–596.

Mak, M., 1991: Dynamics of an atmospheric blocking as deduced from its local energetics. *Quart. J. Roy. Meteor. Soc.,* **117,** 477–494.

——, and M. Cai, 1989: Local barotropic instability. *J. Atmos. Sci.,* **46,** 3289–3311.

Nakamura, H., M. Nakamura, and J. L. Anderson, 1997: The role of high-and low-frequency dynamics in the blocking formation. *Mon. Wea. Rev.,* **125,** 2074–2093.

Nielsen-Gammon, J. W., and R. J. Lefevre, 1996: Piecewise tendency diagnosis of dynamical processes governing the development of an upper-tropospheric mobile trough. *J. Atmos. Sci.,* **53,** 3120–3142.

Orlanski, I., and E. K. M. Chang, 1993: Ageostrophic geopotential fluxes in downstream and upstream development of baroclinic waves. *J. Atmos. Sci.,* **50,** 212–225.

Shutts, G. J., 1983: The propogation of eddies in diffluent jet streams: Eddy vorticity forcing of ''blocking'' flow fields. *Quart. J. Roy. Meteor. Soc.,* **109,** 737–762.

Tracton, M. S., 1990: Predictability and its relationship to scale-interaction processes in blocking. *Mon. Wea. Rev.,* **118,** 1666–1695.

Trenberth, K. E., 1992: Global analyses from ECMWF and atlas of 1000 to 10 mb circulation statistics. NCAR Tech. Note 373 + STR, 191 pp. [Available from the Climate and Global Dynamics Division, National Center for Atmospheric Research, P.O. Box 3000, Boulder, CO, 80307.]

Watson, J. S., 1999: Using time-lagged ensemble forecasts to generate blocking probabilities. M.S. thesis, Department of Earth and Atmospheric Sciences, Cornell University, 106 pp. [Available from the author at 117 Imperial Way, Bayport, NY 11705.]

Downloaded from http://journals.ametsoc.org/doi/pdf/10.1175/1520-0469(2001)058<0933:PSPFTO>2.0.CO;2 by guest on 21 September 2020